Using In situ Capacitance Measurements to Monitor the Stability of Thermal Interface Materials in Complex PCB Assemblies

Michael Gaynes, Timothy Chainer and Edward Yarmchuk
IBM T. J. Watson Research Center
1101 Kitchawan Road
914 945 1838
gaynesma@us.ibm.com
Yorktown Heights, NY 10598
John Torok, David Edwards, David Olson and Katie Pizzolato
IBM Corporation
Poughkeepsie, NY 12601

Abstract

A thermal solution for an array of voltage transformer modules which are cooled by a large area, common aluminum heat spreader for a high end server was evaluated using an in situ, capacitive bond line thermal measurement technique. The method measures the capacitance of a non-electrically conducting thermal interface material (TIM) between the electronic module and heat spreader to quantify the TIM bond line effective thickness during assembly and operation. The thermal resistance of the TIM has the same geometric dependence as the inverse of capacitance, therefore, the capacitive technique also provided a monitor of the thermal performance of the interface.

This technique was applied to measure the bond line in real time during the assembly of the heat spreader to an array of 37 modules mounted on a printed circuit board. The results showed that the target bond lines were not achieved by application of a constant force alone on the heat spreader, and guided an improved assembly process.

The mechanical motion of the TIM was monitored in situ during thermal cycling and found to fluctuate systematically from the hot to cold portions of the thermal cycle, either compressing or stretching the TIM respectively. The capacitive bond line trend showed thermal interface degradation vs. cycle count for several modules which was confirmed by disassembly and visual inspection. Areas of depleted TIM ranged as high as 25% of the module area.

Several design and material changes were shown to improve the TIM stability. Power cycling tests were run in parallel to the thermal cycle tests to help relate the results to field performance. The capacitance technique enabled the development and verification of a thermal solution for a complex mechanical system early in the development cycle.

Key words: Thermal interface materials, heat spreader, capacitance.

Introduction

Heat sinks have been individually attached to a variety of modules on complex printed board assemblies. As packaging integration increases, more design forethought is required to ensure efficient and effective removal of heat from high power electronic modules. More control over air flow is possible when a common heat spreader is interfaced to the various high heat generating modules. Air flow can be directed through channels that are integrated into the heat spreader. There are new challenges when using a common heat spreader. A large area heat spreader that is thermally interfaced to many modules will require greater force to reach the target bond line of the thermal interface material (TIM.) Modules, which could be the same design or a variety of designs, will have different heights above the printed circuit board (PCB.) The TIM should easily accommodate this tolerance in height which typically could be +/- 0.5 mm for a nominal gap of 1.5 mm. Similarly, it should be easy to separate the heat spreader afterwards in the case when one or more modules fail electrical test and require replacement. During the removal of the heat spreader, it is important that the separation forces be low enough to prevent electrically good modules from being damaged. Finally, TIM structural integrity is

required across all modules to provide a reliable thermal path for heat transfer during the life cycle of the product.

An array of voltage transformer modules is being used in the next generation of high end servers. Thirty-seven of these modules are surface mounted to a large PCB that is 380 x 760 mm. A common heat spreader of similar dimensions is mated to the array of modules and secured with several screws to fixed height standoffs. The voltage transformer module has limits to mechanical compressive and tensile forces. In order to stay below these force limits a very low modulus silicone gel TIM was selected. This TIM easily accommodates the target nominal bond line of 1.5 mm, +/- 0.5 mm. Separation forces were < 0.03 MPa. The thermal resistance of 675 C mm^2 /W at a nominal bond line was adequate for the application. There were other TIMs with lower thermal resistance (<350 Cmm^2 /W) which were still reworkable, however, the tensile separation forces exceeded the limit allowed for the module. Initially, thermal pad TIMs were considered, but the compressive forces required to achieve the range of bond lines exceeded the limit allowed for the module.

Studies and experiments were defined to measure and confirm that the bond lines met specifications; that the compressive and tensile forces did not exceed limits; and that the TIM remained in place during thermal and power cycling.

For non-electrically conducting TIMs, electrical capacitance between the module and the heat spreader can provide a direct probe of the bond line thickness and material integrity of the TIM. In this work, capacitance measurements were made of the thermal interface at all process stages, from initial squeeze out, to final bond line and during thermal mechanical stress testing. This technique provides a unique view of a critical part of the thermal path and exposes the effects of mechanical changes in the overall package that dramatically affect the TIM but can be nearly undetectable from outside the package.

Theory

The module and heat spreader form a parallel plate capacitor which has a TIM dielectric between the two plates. For a pair of parallel conductive plates of area, *A*, spaced a distance, *g*, apart, the capacitance, *C*, is given by:

1) $$C = \frac{\varepsilon_r \varepsilon_0 A}{g}$$

where ε_r = 8.85e-12 Farads/meter is the permittivity of free space and ε_0 is the relative dielectric constant of the material between the plates. The inverse dependence on *g* makes capacitance a very useful and sensitive detector for gap measurements, especially at small gaps. Measuring the capacitance for parallel plates with a known spacing filled with the TIM of interest allows one to determine its dielectric constant, ε_r, by solving equation 1. Subsequently, once the dielectric constant is measured, capacitance measurements can be used to calculate an average, effective gap.

In certain circumstances, thermal conductance and capacitance have very similar geometrical and material property dependencies, making capacitance particularly relevant as an indicator of thermal performance. In uniform heat flow, the conductance, *G*, between parallel surfaces with a gap, *g*, filled with a material of conductivity *k*, is given by:

2) $$G = \frac{kA}{g}$$

Comparing equations 1 and 2, one can see that capacitance and thermal conductance both scale as area divided by gap, with dielectric constant playing the same role as material thermal conductivity.

In electronic assemblies, the module and heat spreader thermal conductivities are typically much higher than that of the TIM, but not infinite, so lateral gradients can be significant and the analogy to the electrical situation will be imperfect. Therefore, capacitance cannot be used as a substitute for detailed thermal modeling and measurement of packages. However, overall module to heat spreader capacitance does reflect the average thermal conductance of the TIM material and will track variations in thermal performance of parts. The measurement does not require special thermal test chips so either early development, mechanically good hardware or standard production parts can be monitored. Also, capacitance can be measured much more quickly and with higher precision than thermal resistance, allowing large numbers of parts to be studied which reduces statistical uncertainty in design and process evaluation experiments.

Experimental

Several evolutionary experiments were completed that characterized the response of the design gap for the TIM at every step from initial heat spreader mating, to the structural integrity of the TIM

under cyclic, thermal mechanical strain. These experiments are described and discussed in three phases. Every phase provided new insights that helped define the next set of experiments. Phase one used one assembly to quantify how the TIM gaps develop during heat spreader mating. Also, testing provided an early development look at how the TIM responded to cyclic, thermal mechanical strain induced during thermal cycling, many months before thermal hardware was available. Phase two used 10 assemblies and compared TIM bond lines to design targets. The effectiveness of design changes that resulted from phase one was studied in depth. In phase three experiments, more realistic power cycling was performed and the impact of surfaces introduced as electrodes to make the capacitive bond line measurements was evaluated.

Phase One Experiments

The first experiment was to determine how the bond line developed as a function of mating force, time and engagement of mechanical fasteners. Twenty of the 37 modules were connected with unshielded ribbon cable to make the capacitance measurement. A copper tape with electrically insulating adhesive was applied to the entire surface of each of the 20 modules which provided the first electrode of a parallel plate capacitor. The wires were soldered to an area of overhanging copper tape and carefully routed across the PCB surface, avoiding fastening standoffs and flow channel ribs in the heat spreader. The other ends of the wires were connected to a Scanner which selected the module to be input to a Capacitance meter running at 10 KHz and 1 volt drive. The second electrode of the parallel plate capacitor was the heat spreader which was connected directly to the Capacitance meter. Data acquisition was controlled by a personal computer using BASIC programming and GPIB (General Purpose Interface Bus). As this experiment used unshielded wire , after all the wiring and data logging connections were completed and the heat spreader was placed and secured, the parallel sum of stray and air gap capacitances, $C_{1,}$ was measured at each of the 20 test sites. The TIM was then deposited and the heat spreader was reattached. The total capacitance $C_{2,}$ was measured which is the sum of the stray and TIM capacitance in the gap. Next by subtracting C_1 from $C_{2,}$ we eliminate the stray capacitance contribution but we also need to take into account that we subtracted the air gap capacitance. However, since the TIM gap in its final assembled state is very nearly the same as the air gap in the previous step, the results reduce to equation 3 which has the effect of reducing ε_r by 1 While equation 3 is only accurate when the air and TIM gaps are equal in the final assembled state, this approximation is quite good over a fairly wide range of bond lines. For example, for a bond line 1.5 times greater than the air gap, the error is only about 7%.

3) $$g_{TIM} = \frac{\varepsilon_0 A(\varepsilon_r - 1)}{C_2 - C_1}$$

Capacitance, temperature and time were logged continuously. The mating force applied to the heat spreader was limited to 250 kg which was determined by assuming a uniform loading of all 37 modules to 90% of the compressive limit. Figure 1 is a plot of the TIM bond line vs. time and mechanical loading. The ultimate bond lines were not achieved with 250 kg mating force and time alone. Only after engaging the screws and securing to the standoffs were stable bond lines achieved: 1.2 to 1.7 mm.

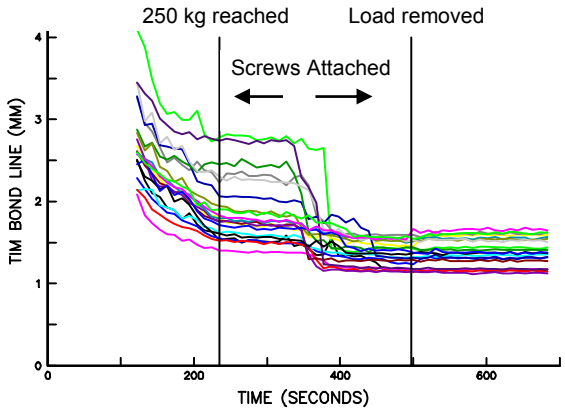

Figure 1: TIM bond line response to load, time and fastening.

Instantaneous loads can be very high when screws are engaged given the typical strain rate dependency of the TIM with respect to stiffness during compression. In order to ensure that the individual compressive loads on voltage converter modules were within the force limits, in situ force measurements were made. A screw fastening sequence and rate were defined to keep the instantaneous loading on any single module in a safe region which eliminated the 250 kg loading process. Several of the bond lines were also measured by leaving out the TIM and placing a sandwich of room temperature curing epoxy between thin release layers on the module surface. The heat spreader was placed when uncured epoxy was in place and it was removed after the epoxy cured. A precision micrometer was used to measure the cured disk of epoxy and the agreement with the bond line calculated from

capacitance was within 10%. One difference in the two measurement methods was that the bond line calculated from capacitance represented the entire area of the module while the epoxy disks covered 5% to 10% of the area in the center.

The next experiment was to monitor the integrity of the TIM in the assembly during thermal cycling. TIM was applied on the heat spreader to all 37 module locations. After the heat spreader was mated and secured with screws, the capacitance was measured 10 times on the bench to ensure that electrical connections were good and that the capacitance readings were stable, typically < 0.01 pF fluctuations. Next, the assembly was moved into the thermal cycle chamber and the capacitance was measured 10 times again. As the heat spreader forms one of the two parallel plate capacitor electrodes and is also electrically connected to the sever ground it was important to electrically isolate the server from earth ground during the measurements. The first 10 thermal cycles were -40 C to 60 C and this represents the temperature extremes that are possible during shipping. Under computer program control, capacitance readings were made on all 20 modules every five minutes. After the 10 shipping thermal cycles, the cycle was changed to 10 to 70 C, representing an over stress, power on/off cycle. Figure 2 shows a typical bond line response vs. temperature cycling. During the cooling portion of the cycle, the bond line increases, indicating that there is a tensile force on the TIM. Conversely, during the heating portion of the cycle, the bond line decreases, indicating that there is a compressive force on the TIM. Total peak to valley TIM movement was measured at roughly 0.18 mm. However, the absolute accuracy of the TIM movement can be affected by several experimental factors. First, the bond line calculation uses the dielectric constant of the TIM which could be changing during the thermal cycle. Secondly, air can be pumped into or out of the bulk TIM under the tensile and compressive loads during the thermal cycle. To further quantify the absolute movement, in a later experiment, gap motion is measured with no TIM present and the dielectric constant of air is used.

The gap motion that is suggested by the 0.18 mm peak to valley estimate is a concern when compared to the results of tensile adhesion testing of individual modules to a heat spreader surface. These samples reached peaked tensile loads at about 0.22 mm elongation on a 1.5 mm bond line. For the 20 modules that were measured, the range in peak to valley movement was < 0.05 mm to almost 0.4 mm. Figure 3 shows the results after almost 500 thermal

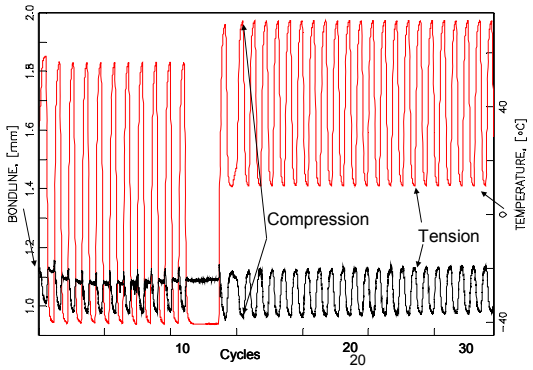

Figure 2: Bond line response to thermal cycling

cycles for a module that had a peak to valley change of < 0.05 mm. The bond line is very stable and the amplitude of motion is not changing with increasing thermal cycles. When the thermal cycle changed from 10-70 C to 10-90 C, bondline compression increases from 70 to 90 C as shown in the plot in Figure 3. Photographs of the heat spreader site and the module after disassembly are shown in Figure 4. The fissures that appear in the TIM on the heat spreader side are an indicator of structure weakness.

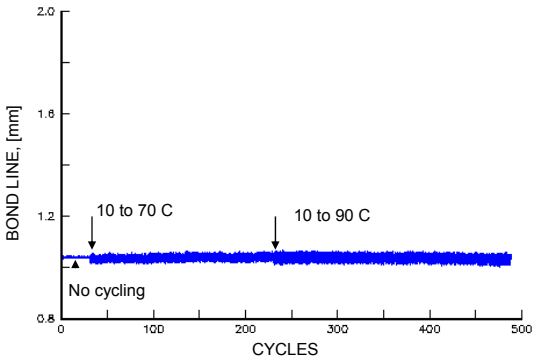

Figure 3: Bond line response of a module to thermal cycling with peak to valley motion < 0.05 mm.

Figure 5 shows the results of the capacitive bond line response for a module that had an initial peak to valley bondline change of almost 0.4 mm. The average bond line was roughly 1.1 mm and increases steadily during thermal cycle testing. At the end of the thermal cycle test, the system was disassembled and the module was visually inspected as shown in Figure 6.

The photo in Figure 6 shows that the TIM is moving or “pumping” out of the gap, which is further confirmed by the observation that the fillet at the top is much larger than the fillet at the bottom in the heat spreader site. The loss of TIM in the gap corresponds to roughly 25% of the TIM area. This reduction of

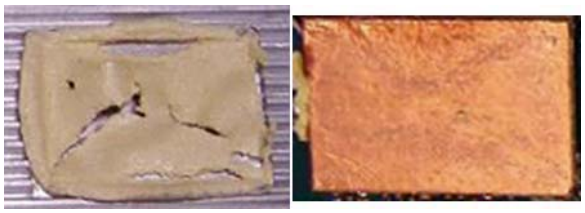

Figure 4: Photos of the residual TIM on the heat spreader location (left) and a module (right) after thermal cycle test.

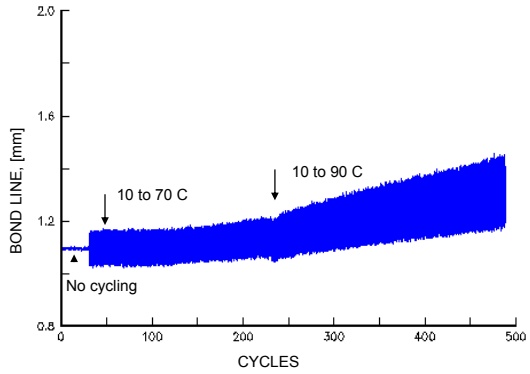

Figure 5: Bond line response of a module to thermal cycling suggesting peak to valley motion ~ 0.4 mm.

TIM in the gap and replacement by air decreases the gap capacitance which per Equation 3 would be calculated as an increasing bond line.

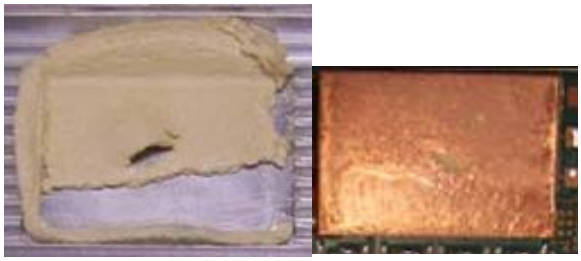

Figure 6: Photos of heat spreader location (left) and a module (right) after thermal cycle test show asymmetric fillets and ~25% loss in TIM area.

Only eight of the 20 sites that were monitored showed a stable capacitive bond line response throughout the thermal cycle testing. Ten sites showed an increasing capacitive bond line which equated to > 15% loss of TIM area and asymmetrical fillets. The TIM movement is due to the cycles of compression during the heating portion of the cycle and tension during the cooling portion. Additional experiments were defined to quantify absolute motion; mitigate the TIM movement; and compare thermal and power cycle induced motion.

Phase Two Experiments

In order to achieve higher accuracy in measuring absolute gap movement either with or without the TIM present, two improvements were made that reduced the stray capacitance an order of magnitude (from 45pF to 4 pF). Instead of using unshielded wire as was done in the Phase One experiments which picked up stray capacitance from the heat spreader, coaxial cable was used. The outer conductor was an electrical shield that blocked the stray capacitance from the heat spreader to the inner conductor which was used to make the capacitance measurement. In addition, two layers of copper tape were used to form the module electrode. A first layer of copper tape on the modules was connected to electrical shield and blocked capacitive coupling from the module and PCB. A second layer of copper tape was placed over the shield layer and was connected to the inner conductor of the coax wire which was connected to a scanner channel. All of the shield wires were electrically interconnected near the Scanner and connected to the shield of the Capacitance meter. The stray capacitance was shown not to change when the heat spreader was assembled due to the shielding. This allowed the stray to be measured without the heat spreader and simply subtracted from the measured values. Further, the stability of the stray capacitance vs. temperature was also measured and shown to be < 0.04 pF worst case, which is an error of < 0.6% for an air gap and < 0.1% for a TIM gap for a bond line of 1 mm.

Figure 7 shows the air gap changes for all modules during a ship shock thermal cycle between -40 C and 60 C. Consistent with the trend in the first test, at the cold temperature, the air gap increases as much as 20 um, and at the hot temperature, it decreases as much as 80 um. The air gap motion was converted to strain for correlation to changes in capacitive bond line of the TIM during thermal cycling and evidence of pumping. The nominal air gap strain was 6%: Figure 8.

Quantifying the gap motion enabled studies on how to reduce or eliminate TIM movement or "pumping." In previous investigations, roughening the heat spreader surface was found to reduce thermal cycling induced movement of thermal greases [1]. Strain controlled, cyclic testing was completed on individual modules mated to heat spreader surfaces and is reported in another paper [2]. Heat spreaders were prepared with N8 and N9 surface finishes. Air gap measurements were made during a thermal cycle between -40 and 60 C. The heat spreader was removed, TIM was deposited onto the surfaces where

the modules mated and it was reattached. The system was thermal cycled with 10 cycles of -40 to 60 C followed by 350 thermal cycles from 10 to 70 C. As before, stray capacitance was measured for every

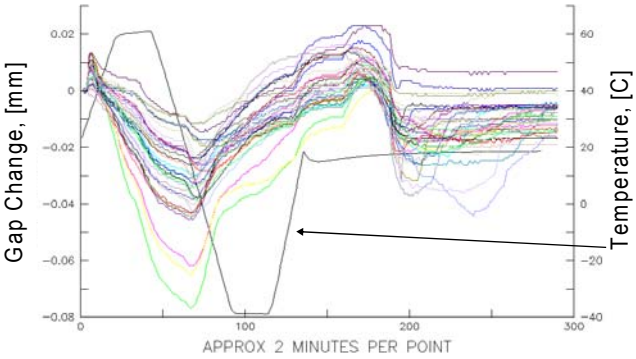

Figure 7: Absolute air gap motion vs. thermal cycle from -40 to 60 C, +20 um and -80 um respectively.

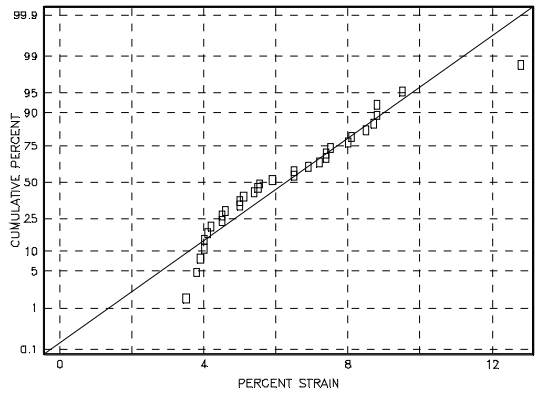

Figure 8: Distribution of strain in air gaps for 32 modules. Nominal strain is six percent.

module before the TIM was deposited so that it could be subtracted from the capacitance measured with the TIM present. Capacitance measurements were made every five minutes on 32 modules.

Figure 9 shows the results for a high strain (8.5%) module site. The capacitive bond line shows an upward trend suggesting some TIM pumping. The photos provide evidence of TIM pumping showing asymmetric fillets and fissures in the TIM. The decrease in capacitance equates to a 3% loss in area.

Figure 10 shows the results for a nominal strain (5.5%) module site. The capacitive bond line is stable, suggesting no significant TIM pumping. The precursors to TIM pumping, asymmetric fillets and fissures in the TIM are evident.

The plot in Figure 11 shows that there is a mild correlation between the air gap strain and the mean shift in capacitive bond line for the 32 modules that were tested.

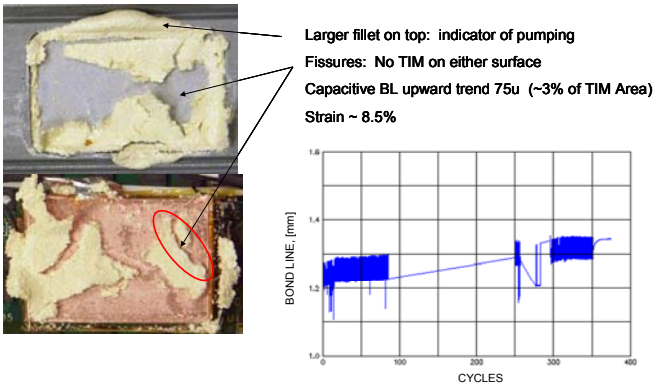

Figure 9: Photos of heat spreader location (top left) and module (bottom left) after thermal cycle test. Capacitive bond line response to air gap of 8.5% strain (right).

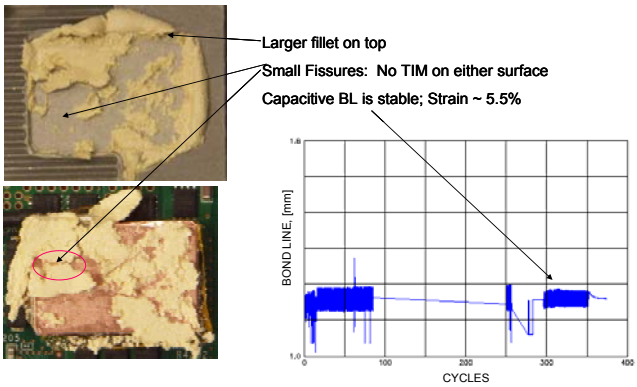

Figure 10: Photos of heat spreader location (top left) and module (bottom left) after thermal cycle test. Air gap strain is 5.5%.

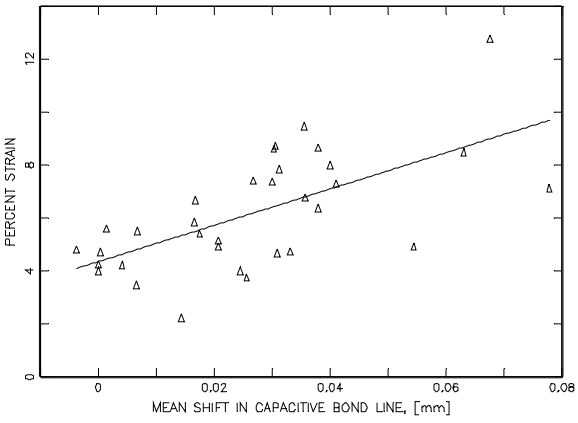

Figure 11: Correlation between strain and mean shift in capacitive bond line: $R^2 = 0.4$.

The results for the roughened heat spreaders were an improvement compared to the first test with the non roughened heat spreader. However, the evidence that there was still a low level of TIM pumping directed further study. One objective was to determine if the copper tape electrodes caused a different response compared to a module without the electrodes. Another objective was to compare thermal cycling to more realistic power cycling.

Phase Three Experiments

The disassembly results after phases one and two showed both cases of TIM pumping and cases of precursors to pumping. These results were used to help interpret the TIM responses when no copper tape electrodes were present during both thermal and power cycling. First, a heat spreader without roughening (smooth) was used and approximately 500 system power-up and down cycles were run. During disassembly, it was observed that 10 out of 37 modules showed no evidence of TIM pumping as represented in Figure 12. However, the other 27 modules had one or more of the signatures of TIM pumping: asymmetric fillets (8), fissures (15), both asymmetric fillets and fissures (4) and 5-15% loss of TIM area (10). Figure 13 shows a typical response with an asymmetrical fillet and a large fissure that represents a loss in TIM area of about 10%. The same assembly was prepared for thermal cycle testing out to 350 cycles. Similar TIM movement occurred in both power cycling (Figure 13) and thermal cycling (Figure 14) when a smooth heat spreader was used and no copper tape electrodes were present.

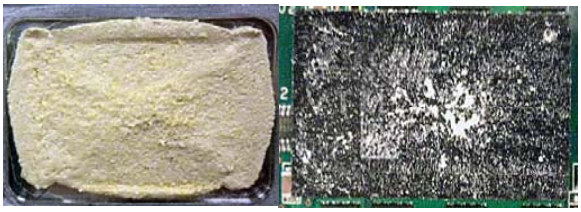

Figure 12: Photos of smooth heat spreader location (top) and module (bottom) after power cycle test. No evidence of TIM pumping is present.

Next, the response for a heat spreader with an N9 surface finish was compared after exposure to 1250 power cycles and more than 1000 thermal cycles, again without any copper tape electrodes. Figures 15 and 16 are photos of typical sites after thermal and power cycling, respectively. In these figures, there is no significant evidence of TIM pumping. On other modules not shown, there are infrequent occurrences of very small fissures that do not add up to any quantifiable loss in TIM area.

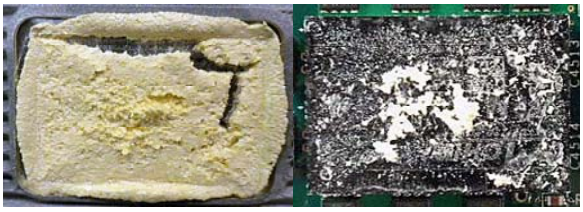

Figure 13: Photos of smooth heat spreader location (top) and module (bottom) after power cycle test. Evidence of TIM pumping is present: larger upper fillet and large fissure.

Figure 14: Photos of smooth heat spreader location (left) and module (right) after thermal cycle test, without any copper electrode. Evidence of TIM pumping is present; ~20% loss in TIM area.

It was concluded that the copper electrodes on the modules do not alter the results of TIM pumping for the smooth (N6/N7) heat spreaders. The benefit of roughening the heat spreader is also evident when the copper electrodes are used. However, the precursor evidence to TIM pumping is nearly completely absent on the assembly that was thermal cycled without copper tape electrodes on the modules. In contrast, 27 out of 37 modules with copper tape electrodes that were thermal cycled showed the precursor signs of TIM pumping. In this test, though, the capacitive bond line was stable on all modules.

Figure 15: Photos of heat spreader (N9) location (left) and module (right) after thermal cycle test, without any copper electrode. No evidence of TIM pumping.

One last test was performed to quantify the gap motion during power cycle and compare to the range of 100 um that was previously measured in

Figure 16: Photos of heat spreader (N9) location (left) and module (right) after power cycle test, without copper electrodes. No evidence of pumping.

thermal cycle. Power cycling was performed with and without TIM. The agreement in the absolute gap measurements that were made with and without TIM, shown in Figure 17 was within 12%. The measurements were less noisy when the gaps were filled with TIM compared to air filled gaps because of the dielectric constant of the TIM providing roughly a 3.5 increase in the capacitance. A measurement of the TIM filled gaps during power cycling is shown in Figure 18 for a typical module. The range in motion of the TIM filled gap during power cycling was only 10 microns which was 10 times lower than the motion measured in thermal cycling of 100 microns.

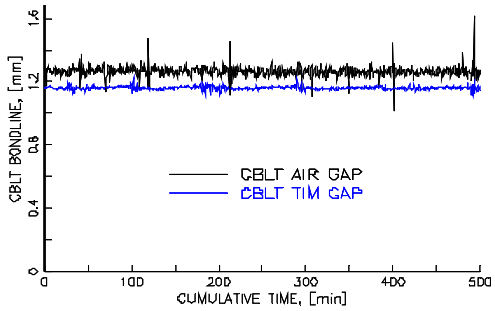

Figure 17: Capacitive gap measurements during power cycling are consistent with and without TIM.

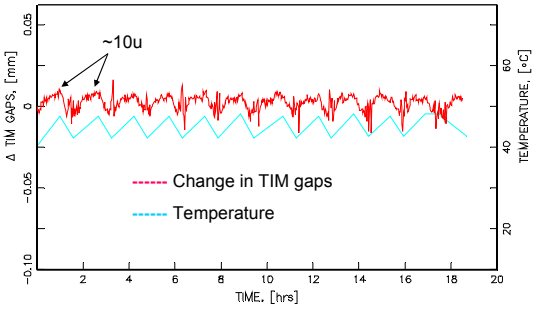

Figure 18: TIM gap motion vs. power cycle.

Summary

Assemblies with a smooth heat spreader experience increasing capacitive bond line during thermal cycle testing equivalent to as much as 25% of area loss in TIM. TIM pumping occurs with and without copper tape electrodes during thermal cycling and without copper electrodes during power cycling. (Extended power cycling was not done with copper electrodes on the module surfaces.)

Assemblies with an N9 heat spreader and copper tape electrodes have a more stable capacitive bond line and equivalent area losses in TIM are less than 5%. Precursors to TIM pumping are evident: fissures and asymmetric fillets

Assemblies with an N9 heat spreader but without copper tape electrodes have very few and small fissures after both thermal and power cycling. No quantifiable area loss in TIM is observed.

The range of motion in power cycling is a factor of 10 less than in thermal cycling.

The combined benefits of the roughened heat spreader surface and the order of magnitude less gap motion in power cycling compared to thermal cycling provide confidence that thermal performance will be maintained under operational life. Monitoring the response of the TIM with capacitance is easy and provides timely insight throughout the development cycle. Confidence can be gained on the reliability of the thermal solution well before thermal hardware is available for final system level thermal test.

Acknowledgements

We thank Ron Spulverino for wiring the assemblies for capacitance measurements.

References

[1] Iruvanti, S., Klepeis, M., Messina, G., and Sherif, R., “Integral Mesh Plate Cooling Module”, US Patent 5,825,087, October 20, 1998.

[2] Doman, J., Kobeda, E., Bielick, J., Kuczynski, J., Tofil, T., and Vaughn, M., “Evaluation of Thermal Interface Material Performance in a Cyclic Strain Environment”, Proceedings of the Surface Mount Technology Association, International (SMTAi) Conference, Orlando, Florida, October 24-28, 2010.